

Forest health and vitality: the detection and monitoring of *Pinus patula* trees infected by *Sirex noctilio* using digital multispectral imagery

R Ismail*, O Mutanga and U Bob

Department of Geography and Environmental Studies, University of KwaZulu-Natal, Private Bag X01, Scottsville 3209, South Africa

* Corresponding author, e-mail: riyad.ismail@sappi.com

The Eurasian woodwasp, *Sirex noctilio*, causes considerable tree mortality in commercial pine plantations in southern KwaZulu-Natal, South Africa. Broad-scale visual assessments of infestation provided by forest managers are currently used to measure forest health and vitality. The effectiveness of visual assessments is questionable because they are qualitative, subjective and dependent on the skill of the surveyor. Remote sensing technology provides a synoptic view of the canopy and thus offers an alternative to the conventional methods of monitoring forest health and vitality. In this study, high resolution (0.5 × 0.5m) digital multispectral imagery (DMSI) was acquired over commercial *Pinus patula* trees of varying age classes, which had been ground assessed and ranked on an individual tree crown basis using a severity scale. The severity scale was based on a hierarchy of decline symptoms that are visibly apparent on the infested tree and are represented in this study as the green, red and grey stages. A series of ratio- and linear-based vegetation indices were then calculated and compared to the different crown condition classes as determined by severity scale. Of the vegetation indices derived from the high-resolution DMSI, significant differences between the pre-visual (healthy and green stages) and visual (red and grey stages) crown condition classes were obtained. Canonical variate analysis further revealed that greater discriminatory power between the different crown condition classes is obtained when using the normalised difference vegetation index (NDVI). Overall the study demonstrated the potential benefit of using high-resolution DMSI to discriminate between healthy trees and trees that were in the visual stage of infestation.

Keywords: digital multispectral imagery, remote sensing, *Sirex noctilio*, vegetation indices

Introduction

There are approximately 1.5 million ha of commercial forest in South Africa (Zwolinski *et al.*, 1998) with forest products contributing 1.2% (approximately R14 billion) to the gross domestic product (GDP) of the country (DWAf, 2004). The industry depends almost exclusively on the planting of exotic *Pinus*, *Eucalyptus* and *Acacia* species (van Staden *et al.*, 2004). However, emerging evidence suggests that new pests and pathogens are appearing at an increasing rate and could potentially impact on the future sustainability of the industry (Wingfield *et al.*, 2001). *Sirex noctilio* (Fabricius), which was first detected in 1994 in the Western Cape (Tribe, 1995; Tribe and Cillie, 2004), is currently causing considerable tree mortality in commercial forest plantations in southern KwaZulu-Natal. In an effort to minimise the potential threat of *S. noctilio* to commercial pine production in the region, an integrated management strategy combining detection and monitoring methods, silvicultural treatments and biological controls has been implemented on an industry-wide basis in South Africa (Ismail *et al.*, 2006).

The primary control of established *S. noctilio* populations is achieved by biological means using the nematode *Deladenus siricidicola* (Bedding) and parasitic wasps such as *Ibalia leucospoides* (Hochenwarth) and *Megarhyssa*

nortoni (Cresson), while silvicultural methods such as thinning are carried out to improve tree vigour and thereby keep damage within acceptable levels (Haugen *et al.*, 1990; Ismail *et al.*, 2005). However, successful implementation of the above control measures depends on our ability to spatially quantify the severity and extent of infestation so that forest managers can adopt the most appropriate course of intervention before the stand reaches a point of non-recovery. Additionally, geographic information systems (GIS) and forest planning systems, which include harvesting schedules, timber volume analysis and species growth models, have been developed to help foresters manage infected areas. These systems require accurate spatial information on the severity and extent of *S. noctilio* damage. Current methods used to spatially identify the severity and extent of *S. noctilio* infestation includes broad-scale visual aerial reconnaissance followed by field-based exercises to verify the results. Although visual assessments of infestation are widely used to measure forest health (Haara and Nevalainen, 2002), the effectiveness of visual assessments are questionable because they are qualitative, subjective and dependent on the skill of the surveyor (McConnell *et al.*, 2000; Stone and Coops, 2004).

Internationally, the use of remote sensing technology to detect, monitor and map forest health over large areas has been a subject of great interest, resulting in the testing of a variety of airborne remote-sensed data, such as high spatial resolution digital multispectral imagery (DMSI) (Leckie *et al.*, 2005), hyperspectral scanners (Coops *et al.*, 2003) and video recorders (Yuan *et al.*, 1991). The limited potential of satellite-based methods is primarily due to the short time available for detection and the different responses at needle, branch and canopy scales (Radeloff *et al.*, 1999). In general, the monitoring and detection of forest damage using remote sensing has been limited to three classes of infestations (light, medium and heavy) with accuracies ranging between 70% and 80% (Radeloff *et al.*, 1999). Similar accuracies were reported in Canadian case studies that used remote sensing to survey the impacts of mountain pine beetle (Wulder and Dymond, 2004).

Compared to traditional methods, the commercial availability of DMSI in South Africa offers a potential source for the effective collection of spatially accurate, consistent and timely imagery regarding the impacts of *S. noctilio* at the compartment level. High-resolution DMSI (pixel sizes less than 1 × 1 m) is capable of achieving higher mapping accuracies by identifying individual crowns. This is particularly useful because pine plantations infested by *S. noctilio* have a scattering of dead and dying trees (Haugen *et al.*, 1990; Haugen and Underdown, 1990) and there is a need to identify small clusters or individual trees remotely. Additionally, the advantage of using airborne DMSI is the capacity to mobilise quickly at opportunistic times and at user specified locations (Wulder *et al.*, 2004). This is an important benefit for the monitoring of forest health and vitality because infection is often linked to other events, such as climate, disturbance, phenology of forest type and infecting agent (Stone and Coops, 2004). As a result, the date for image acquisition is important in maximising the discriminating potential of classification algorithms (Coops *et al.*, 2003).

This study advocates the use of high spatial resolution DMSI and vegetation indices (VI) to provide a quantitative spatial framework for the detection and monitoring of *Pinus patula* trees infected by *S. noctilio*. The reason for using remotely sensed VI includes the removal of variability caused by canopy geometry, soil background, sunview angles and atmospheric conditions (Gilabert *et al.*, 2002). Additionally, a number of VI have been used successfully to assess changes in the reflectance due to the declining health status of the tree (Leckie *et al.*, 2004; Stone and Coops, 2004). For the purpose of this study we have divided VI generally into two categories, i.e. ratio-based indices and linear-based indices (for a complete review of VI see Jackson and Huete, 1991; Thenkabail *et al.*, 2002).

To the best of our knowledge, no research has examined the use of remote sensing technology for the detection and monitoring of *Pinus patula* trees infected by *S. noctilio*. We examined if VI derived from high-resolution (0.5 × 0.5m) DMSI could characterise stress induced by *S. noctilio* in *P. patula* compartments. We then tested the relative strength of various ratio- and linear-based vegetation indices in discriminating the crown condition classes (healthy, green, red and grey) associated with *S. noctilio* infestations. The

overall objective of this study is to test remotely sensed VI that could assist in detection of *S. noctilio* infestations. Once operational, these techniques could improve our ability to map infested pine compartments more effectively.

Materials and methods

Description of the study area

The study area is approximately 1 750ha and forms part of the Sappi Pinewoods plantation, which is dominated by *P. patula* compartments (Figure 1). The site is located approximately 30km west of the town of Pietermaritzburg, KwaZulu-Natal, South Africa. The average altitude for the site is 1 190m with an average air temperature of 16.1°C (MacFarlane, 2004). The mean annual rainfall of the area is 916mm. The terrain consists of low mountains and undulating hills. The geology of the area is a mixture of mudstone, sandstone, tillite, amphotite and basalt. Soils in the area are mostly sandy-clay and sand-clay loams (MacFarlane, 2004).

Description of the severity scale

Early evidence of *S. noctilio* attack (the green stage) includes the appearance of resin droplets and the presence of ovipositors on the bark with a dark fungal stain appearing along the cambium (Neumann and Minko, 1981; Tribe and Cillie, 2004). There is minimal needle loss and the canopy appears green and healthy. The red stage occurs later when the canopy of the attacked tree changes colour from green to yellow to reddish brown (Ciesla, 2003). Ultimately, during the grey stage, the tree canopy is completely defoliated and round exit holes appear on the bark (Neumann and Minko, 1981). A new generation of adult wasp emerges resulting in a compartment with a scattered pattern of dead or dying trees (Ciesla, 2003; Haugen *et al.*, 1990; Haugen and Underdown, 1990). During the grey stage of attack the wood is totally desiccated (Haugen and Underdown, 1990), the timber is not utilisable and economic losses are incurred. Figure 2 provides a description of the severity classes that were used in this study.

Data acquisition

High-resolution (0.5 × 0.5m) DMSI was acquired on 9 September 2005 (10:00 GMT) by Land Resources International (LRI) Inc, Pietermaritzburg, South Africa with their LrEye aerial imaging system. The LrEye sensor is composed of a series of four monochrome Sony cameras. Each camera collects data for one of the spectral bands shown in Table 1. The resulting four bands were registered using Erdas Imagine (Leica Geosystems, 2004) to form an image with four coregistered spectral bands that are referenced to the Gauss conformal projection (central meridian: 31).

Field data collection took place one week after the image was acquired. A stratified random sampling technique (Richards, 1993) was adopted for this study. The strata were based on the age and occurrence of *P. patula*. Compartments that were harvested, or that were recently planted, were excluded from the sample. A 50 × 50m grid was generated over the study area and ten grid cells were

randomly selected from each predetermined age stratum (i.e. less than seven years, from 8–9 years, 10–12 years and older than 13 years). This age stratification was adopted because it reflects current *S. noctilio* management guidelines. At the centre point of each grid cell, a 10m circular plot was created. Tree crowns located within each plot were manually identified on the LrEye imagery and subsequently located in the field using a Global Positioning System (GPS). In total, 782 trees were assessed for *S. noctilio* infections based on the severity scale that is shown in Figure 2. This process was undertaken with the assistance of Sappi foresters and technical staff who have a detailed understanding of the identification and classification of *S. noctilio* infestations. Additionally, *P. patula* trees that were classified as red-stage infestations were sampled destructively to evaluate the presence or absence of larvae.

Evaluation of vegetation indices

According to Coops *et al.* (2003), the method used to obtain the spectral values of individual trees when using high-resolution imagery is important because significant variation in brightness exists depending on the pixel position within the crown. In a study conducted by Leckie *et al.* (1992) to account for effects of the variation on individual crown delineation it was concluded that either the whole tree or the sunlit tree sampling methods were the most suitable methods to derive consistent and representative spectral response. In this study, the whole crown method was used whereby each of the selected crowns was manually delineated on the LrEye imagery and the crown spectral response extracted for the ratio- and linear-based indices.

Ratio-based indices

It has been reported that plants under stress display a decrease in canopy reflectance in the lower portion of the near infrared, a reduced absorption in the chlorophyll active band and subsequently a shift in the red edge (Carter and Knapp, 2001). Ratio-based indices have been successfully used to assess changes in the reflectance due to the declining health status of a tree (Ekstrand, 1994; Nelson, 1983; Vogelmann, 1990) because they operate by contrasting the intense chlorophyll pigment absorption in the red portion against the high reflectance in the NIR portion of the electromagnetic spectrum (Elvidge and Chen, 1995). The most widely used ratio-based indices such as the ratio vegetation index (RVI) (Jordan, 1969), normalised difference vegetation index (NDVI) (Rouse *et al.*, 1973), difference vegetation index (DVI) (Tucker, 1979) and green normalised difference vegetation index (GNDVI) (Gitelson and Merzlyak, 1998) respond to these differences in the near infrared and visible regions (Lillesand *et al.*, 2004). Table 2 shows the various ratio-based indices that were used in the study.

Linear-based indices

The tasseled cap transformation (TCT) transforms the original spectral bands of a sensor into linear-based indices (Jackson, 1983). Several studies using remotely sensed imagery (Collins and Woodcock, 1996; Healey *et al.*, 2005; Jin and Sader, 2005; Price and Jakubauskas, 1998; Sharma and Murtha, 2001; Skakun *et al.*, 2003) have

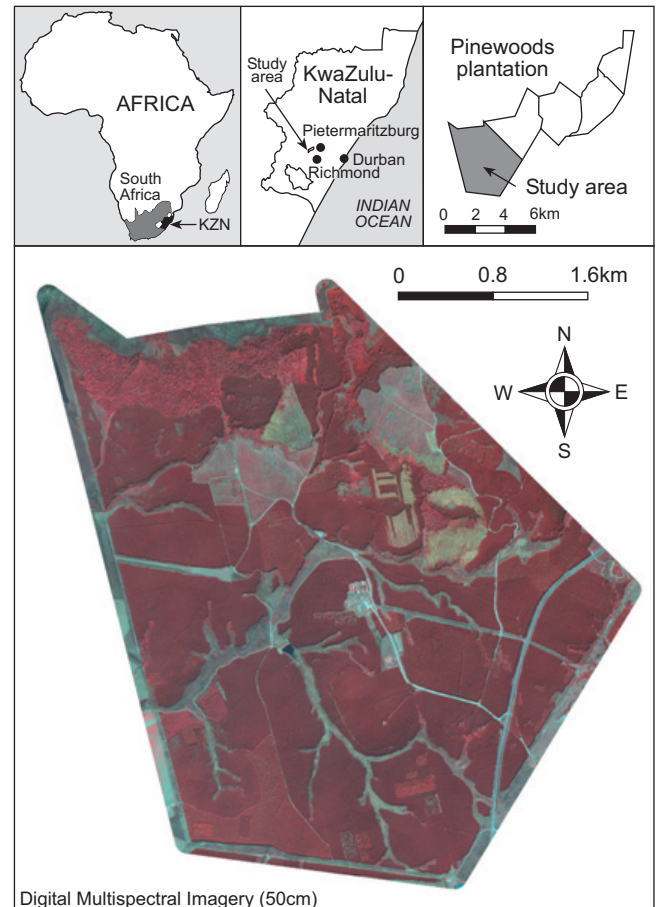


Figure 1: Location of the study area

shown the value of using the linear indices when assessing forest health and vitality. This is largely due to the fact that colour changes (chlorosis) associated with damaged trees is organised along the principal directions of the newly created linear-based indices (Skakun *et al.*, 2003).

The Gram-Schmidt orthogonalisation process was used to derive the TCT coefficients for the linear-based indices (Jackson, 1983). Initially, a soil line and the vector in the brightness direction are determined; subsequently, from the brightness vector all other vectors (greenness and yellowness) are orthogonally calculated. Coefficients (Table 3) are based on the grey level values of four land cover types (wet soil, dry soil, green vegetation and senesced vegetation) found on the imagery. Water was used to represent wet soil values because pixels representing wet soils were not found in the imagery (Gong *et al.*, 2003). Dry soil values were collected from dirt roads and healthy tree crowns represented green vegetation. Dry grass values were used to represent senesced vegetation. Yarbrough *et al.* (2005) and Jackson (1983) provide a detailed mathematical description for calculating coefficients for n space indices using the Gram-Schmidt orthogonalisation process.

The resulting linear equations for brightness, greenness and yellowness are as follows:

Brightness (TCB) = 0.337663 (blue) + 0.586272 (green) + 0.638220 (red) + 0.367348 (NIR)
 Greenness (TCG) = -0.227113 (blue) - 0.131965 (green) - 0.288569 (red) + 0.920724 (NIR)
 Yellowness (TCY) = 0.097931 (blue) - 0.781721 (green) + 0.607311 (red) + 0.102451 (NIR)

Statistical analysis

Firstly, analysis was undertaken to compare the capacity of ratio- and linear-based indices to discriminate between each of the crown condition classes (Figure 2). This was tested using an analysis of variance (ANOVA) with a Tukey's HSD post hoc analysis (Coops *et al.*, 2003).

Class	Stage	Crown condition		Symptoms
1	Previsual	Healthy		No signs of <i>S. noctilio</i> infestation
2	Previsual	Green		Green crown, presence of resin droplets, cambium stain, ovipositors found on the trunk and no needle loss
3	Visual	Red		Severe chlorosis, reddish brown canopy and high needle loss
4	Visual	Grey		Emergence holes, no canopy, most branches intact and 100% needle loss

Figure 2: Description of the severity classes used for ground assessment of *Sirex noctilio* infestations

Table 1: Spectral range of Landsat TM compared to the LrEye sensor

Band	Colour	Landsat TM spectral range (nm)	Landsat TM spatial range (m)	LREye spectral range (nm)	LREye spatial range (m)
1	Blue (B)	450–520	30	450–480	0.5
2	Green (G)	520–600	30	550–580	0.5
3	Red (R)	630–690	30	650–680	0.5
4	Near Infrared (NIR)	760–900	30	850–900	0.5

Secondly, canonical variate analysis (CVA) was used to determine which single VI best discriminated against the crown condition classes. CVA is a multivariate statistical technique that discriminates among prespecified groups of sampling entities based on a suite of characteristics (McGarigal *et al.*, 2000). The technique involves deriving linear combinations (i.e. canonical functions) of two or more discriminating variables that will best discriminate among the *a priori* defined groups (Mutanga, 2005). In this study, VI are entered into the analysis based on their ability to increase group separation (i.e. crown condition classes). This reduces the number of indices to a subset that provides the best discrimination among classes. The best linear combination of VI is achieved by the statistical decision rule of maximising the among-group variance, relative to the within-group variance (Mutanga, 2005). The first discriminant function provides the best separation among classes, while the second function separates classes using information not used in the first function and so forth. Additionally, the functions will be independent or orthogonal, that is, their contributions to the discrimination between groups will not overlap (Lawrence and Labus, 2003).

Finally, we used the leave-one-out cross-validation technique ($n = 782$) for estimating the error rate conditioned on the training data (Mutanga, 2005). The advantage of using the leave-one-out cross-validation technique is that all the data is used for estimating error. Using this technique, each observation is systematically removed, the canonical function re-estimated and the excluded observation classified (Mutanga, 2005). A confusion matrix is then constructed to compare the field (true) crown condition classes with the class assigned by the VI to the sample dataset. It depicts accuracies of the crown condition classes (producer's and user's accuracies). Producer accuracies are calculated by dividing the number of correctly classified trees in each crown condition class by the number of training data used for that class (i.e. column total in the confusion matrix). User accuracies are computed by dividing the number of correctly classified trees by the total number of trees that were classified in that crown condition class (i.e. row total

in the confusion matrix). Additionally, a discrete multivariate technique called kappa analysis that uses the k (KHAT) statistic as a measure of agreement with the reference data was calculated (Congalton and Green, 1999; Skidmore, 1999). This statistic serves as an indicator of the extent to which the percentage correct values of an error matrix are due to 'true' agreement versus 'chance' agreement (Lillesand *et al.*, 2004). If the kappa coefficients are one or close to one, there is perfect agreement between the training and test data.

Results

We tested the hypothesis that ratio- and linear-based vegetation indices would discriminate among the various crown condition classes by conducting a one-way ANOVA. Of the vegetation indices calculated, significant differences ($p < 0.001$) were obtained using NDVI, GNDVI, DVI, RVI, TCG and TCB. A one-way ANOVA shows that there is a significant difference between the vegetation indices and the crown condition classes, but it does not show which crown condition classes are different. We therefore executed a Tukey's HSD post hoc test in order to establish differences between each of the crown condition classes (healthy, green, red and grey). Results with their respective level of significance are shown in Table 4.

Both the ratio- (NDVI, RVI, DVI and GNDVI) and linear-based indices (TCB and TCG) are poor at discriminating between classes 1 (healthy) and 2 (green stage). However, the VI tested are capable of discriminating between the previsual (classes 1 and 2) and visual (classes 3 and 4) crown condition classes. The most significant degree of separation occurs between class 1 and classes 3 and 4, and between class 2 and classes 3 and 4. All indices are capable of discriminating between these classes except for TCB, which can only discriminate between class 1 and class 4, and between class 2 and class 4. Based on the results from ANOVA, it is difficult to determine which VI has the best discriminatory power. Therefore, we carried out a canonical variate analysis and included all indices

Table 2: Ratio-based vegetation indices used in this study

Vegetation index name	Index	Equation	Reference
1 Normalised difference vegetation index	NDVI	$NDVI = (NIR - red)/(NIR + red)$	Rouse <i>et al.</i> (1973) Jackson (1983)
2 Ratio vegetation index	RVI	$RVI = NIR/red$	Jordan (1969)
3 Difference vegetation index	DVI	$DVI = NIR - red$	Tucker (1979)
4 Green normalised difference vegetation index	GNDVI	$GNDVI = (NIR - green)/(NIR + green)$	Gitelson and Merzlyak (1998)

Table 3: Gram-Schmidt coefficients

	B	G	R	NIR
Brightness (TCB)	0.337663	0.586272	0.638220	0.367348
Greenness (TCG)	-0.227113	-0.131965	-0.288569	0.920724
Yellowness (TCY)	0.097931	-0.781721	0.607311	0.102451

Table 4: Analysis of variance results with a Tukey's HSD post-hoc test. Class: 1 = healthy, 2 = green, 3 = red and 4 = grey

NDVI	1	2	3	4	TCG	1	2	3	4
1	..	**	*	*	1	..	**	*	*
2	**	..	*	*	2	**	..	*	*
3	*	*	..	*	3	*	*	..	*
4	*	*	*	..	4	*	*	*	..
GNDVI	1	2	3	4	TCB	1	2	3	4
1	..	**	*	*	1	..	**	**	*
2	**	..	*	*	2	**	..	**	*
3	*	*	..	*	3	**	**	..	**
4	*	*	*	..	4	*	*	**	..
DVI	1	2	3	4	NIR	1	2	3	4
1	..	**	*	*	1	..	**	*	*
2	**	..	*	*	2	**	..	*	*
3	*	*	..	*	3	*	*	..	*
4	*	*	*	..	4	*	*	*	..

* Not significant; ** $p < 0.001$

(discriminatory variables) except for the TCB component. Additionally, to improve the discriminatory power of the VI, class 2 (green stage) was grouped with class 1 (healthy trees) while the rest of the classes remained the same, i.e. class 3 (red stage) and class 4 (grey stage).

Canonical variate analysis (CVA)

We tested the relative strength of various ratio- and linear-based vegetation indices in detecting *S. noctilio* infestations by carrying out a canonical variate analysis (CVA). Table 5 shows the eigenvalues as well as the factor structure matrix from the canonical variate analysis using three crown condition classes (i.e. healthy, red and grey stages). The measure of information contained in the functions is represented by the eigenvalues corresponding to those functions. The eigenvalues are interpreted as the ratio of variances along each function (Richards, 1993). The largest portion of the explained variance (97.5%) is contained in the first canonical function and the remainder is contained in the second function (2.5%).

The factor structure coefficients contained in the matrix represent the correlations between the variables and the canonical functions and are used to interpret the canonical functions (McGarigal *et al.*, 2000). Results indicate that the highest factor structure coefficients are contained in the NDVI (0.633) and the GNDVI (0.629). The second canonical function also shows that one of the largest contributions is contained in the GNDVI (0.605) and to a lesser extent NDVI (0.369); however, the magnitude for the second canonical function is much smaller than that of the first canonical function. The classification accuracy based on the highest factor structure (NDVI) is shown in Table 6.

Discussion

High-resolution DMSI provides a useful and robust tool to improve our ability to detect and monitor *P. patula* trees infected by *S. noctilio*. Ratio- (NDVI, RVI, DVI and GNDVI) and linear-based vegetation indices (TCG) derived from

Table 5: Factor structure matrix representing the correlation between variables and canonical functions (three classes)

	Function 1	Function 2
NDVI	0.633	0.369
GNDVI	0.629	0.605
DVI	0.559	0.550
TCG	0.500	0.669
NIRR	0.484	0.463
Eigenvalue	0.961	0.025
% Variance	97.5	2.5

Table 6: Confusion matrix showing the NDVI predicted accuracy of *Sirex noctilio* infestations using a three-level classification system: class 1 (healthy), class 2 (red) and class 3 (grey)

Class	1	2	3	UA
1	695	2	2	99.43
2	8	26	3	70.27
3	2	3	11	68.75
PA	98.58	83.87	68.75	
KHAT	0.79			

high-resolution DMSI are able to significantly ($p < 0.001$) discriminate between the previsual (healthy and green) and the visual stages of infestations (red and grey). Canonical variate analysis further reveals that greater discriminatory power between the different crown condition classes (Figure 2) is obtained when using NDVI as compared to the other vegetation indices derived from high-resolution DMSI. Accuracy assessments (Table 6) show that NDVI derived from high-resolution DMSI is successful in locating and predicting the condition of tree crowns on the imagery when crown condition classes are reduced to a three classification system, in which case producer accuracies range from 84% (red stage) to 69% (grey stage). The results obtained from this study are comparable to previous international studies on

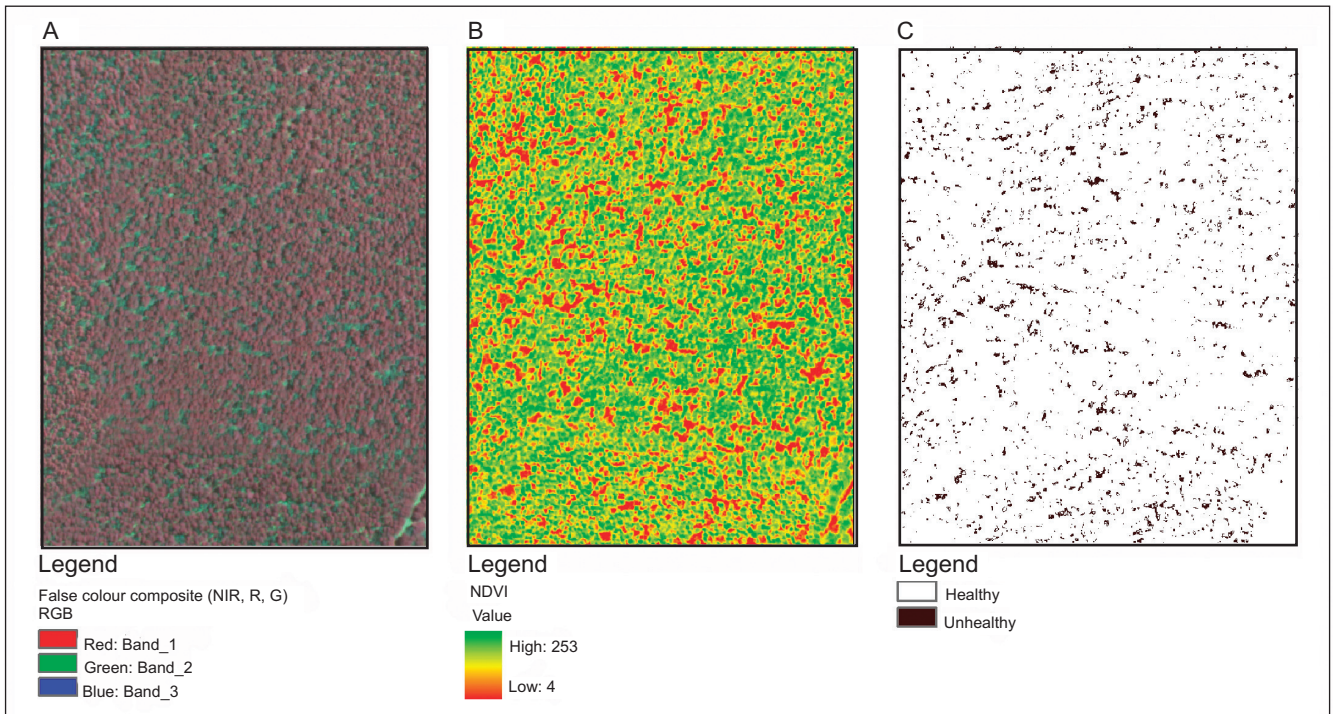


Figure 3: Process flow showing the operational use of remote sensing technology for the detection and monitoring of *Sirex noctilio* red-stage infestations. **A**, 4 band, high-resolution (50cm) DMSI; **B**, calculated NDVI image; and **C**, map of *Sirex noctilio* infestations based on reclassified NDVI values

declining forest health (Vogelmann, 1990; Leckie *et al.*, 2004; Wulder *et al.*, 2004; Leckie *et al.*, 2005) and emphasise the importance of the visible and NIR bands when studying the effects of declining forest health, especially when infestation results in foliar discoloration (red stage).

Detecting and monitoring the red stage of infestation is regarded as a priority among forest managers because it gives an accurate indication of the severity and extent that is taking place that year (i.e. current infestation) (Leckie *et al.*, 2005). Additionally, using high-resolution DMSI to map out the red stage of infestation provides us with a spatial framework that allows for the repetitive and cost-effective monitoring over large areas. This improves our ability to quantify the severity and extent of *S. noctilio* infestations thereby allowing forest managers to design the most appropriate intervention measures. For example, moderate red-stage *S. noctilio* infestations (<10%) would require the inoculation of infested trees with nematodes, whereas heavy infestations (between 10 and 50%) would require sanitisation and salvage operations to be implemented (Haugen *et al.*, 1990; Haugen and Underdown, 1990). Figure 3 shows the process flow when using high-resolution DMSI to quantify red-stage *S. noctilio* infestation spatially.

The difficulty in discriminating the green stage of infestation is consistent with other studies that have attempted to classify light to moderate symptoms using high-resolution remotely sensed imagery (Leckie *et al.*, 2004; Leckie *et al.*, 2005). The success of discriminating green-stage infestation is dependent on the detection of subtle changes in the spectral reflectance of the tree (Ekstrand, 1994). Slight

changes in the spectral reflectance of stressed vegetation, when measured by various broad-band sensors, are often masked by the high degree of variation in reflectance caused by factors such as varying view geometry, illumination and canopy density (Runesson, 1991). Additionally, in commercial forestry this is further impacted by silvicultural operations. Given these limitations, hyperspectral remote sensing offers possibilities to investigate the early stages of infestations based on narrow bands using the entire electromagnetic spectrum. These narrow bands allow for the detection of detailed features that would otherwise have been masked (Schmidt and Skidmore, 2001). This study is part of an ongoing research project and a future objective includes the use of high spectral resolution data to differentiate between the healthy and green stages.

Previous studies (Collins and Woodcock, 1996; Skakun *et al.*, 2003) found changes in the tasseled cap wetness component (TCW) to be a good indicator of conifer mortality and the most consistent indicator of forest change due to the inclusion of the short-wave infrared (SWIR) band. In this study the calculations of the tasseled coefficients were limited to four spectral bands found in the visible and NIR parts of the spectrum (400–900nm) and therefore only included the TCB, TCG and TCY and not the TCW. Additionally, spectrometer research conducted by Leckie *et al.*, (1988) regarding discoloration caused by the spruce budworm indicated that the SWIR regions are better than the visible and NIR for discrimination. Similarly, initial attack by *S. noctilio* changes the water balance of the attacked tree (Neumann and Minko, 1981; Slippers *et al.*, 2003), so

using a sensor that captures SWIR wavelength has the potential to improve overall classification accuracy as well as discrimination between crown condition classes.

Conclusions

This study has shown that NDVI calculated from high spatial resolution DMSI has the potential to detect and monitor canopy damage caused by *S. noctilio*. Although it was difficult to discriminate between the healthy and green stages of infestation, classification accuracies are improved when using a three-class crown condition index that differentiates between the healthy, red and grey stages of infestation. Overall the study demonstrated the potential benefit of using high-resolution DMSI to discriminate between healthy trees and trees that were in the visual stage of infestation. More importantly, this has led to the development of a spatial monitoring framework that is capable of augmenting traditional detection and monitoring methods.

Acknowledgements — Funding for this research was provided by the National Research Foundation (NRF). The digital multispectral imagery (DMSI) for this research was provided by Sappi Forests. We thank Marcel Verleur, Deane Bethell, James Thorpe and Nic Tait for advice throughout the project and Craven Naidoo (Cartographic Unit, University of KwaZulu-Natal) for assisting with the fieldwork. We also thank the referees for valuable comments on the paper.

References

- Carter GA and Knapp AK** (2001) Leaf optical properties in higher plants: linking spectral characteristics to stress and chlorophyll concentration. *American Journal of Botany* 88: 677–684
- Ciesla WM** (2003) European woodwasp: a potential threat to North America's conifer forests. *Journal of Forestry* 18–23
- Collins JB and Woodcock C** (1996) An assessment of several linear change detection techniques for mapping forest mortality using multitemporal Landsat TM data. *Remote Sensing of the Environment* 56: 66–77
- Congalton RG and Green K** (1999) *Assessing the accuracy of remotely sensed data: principles and practices*. Mapping Sciences Series. Lewis Publishers, Boca Raton. 137 p
- Coops NC, Stanford M, Old K, Dudzinski M, Culvenor DS and Stone C** (2003) Assessment of Dothistroma needle blight of *Pinus radiata* using airborne hyperspectral imagery. *Phytopathology* 33: 1524–1532
- DWAF** (2004) *Commercial timber resources and primary roundwood processing in South Africa 2002/2003*. Department of Water Affairs and Forestry, Pretoria
- Ekstrand S** (1994) Assessment of forest damage with Landsat TM: correction for varying forest stand characteristics. *Remote Sensing of the Environment* 47: 291–302
- Elvidge CD and Chen Z** (1995) Comparison of broad-band and narrow band red and near infrared vegetation indices. *Remote Sensing of the Environment* 54: 38–48
- Gilbert MA, Gonzalez-Piqueras J, Garcia-Haro FJ and Melia J** (2002) A generalized soil-adjusted vegetation index. *Remote Sensing of the Environment* 82: 303–310
- Gitelson A and Merzlyak M** (1998) Remote sensing of chlorophyll concentration in higher plant leaves. *Advances in Space Research* 22: 689–692
- Gong P, Mahler S, Biging G and Newburn D** (2003) Vineyard identification in an oak woodland landscape with airborne digital camera. *International Journal of Remote Sensing* 24: 1303–1315
- Haara A and Nevalainen S** (2002) Detection of dead or defoliated spruces using digital aerial data. *Forest Ecology and Management* 160: 97–107
- Haugen DA, Bedding RA, Underdown MG and Neumann FG** (1990) National strategy for control of *Sirex noctilio* in Australia. *Australian Forest Grower* 13(2): 8
- Haugen DA and Underdown MG** (1990) *Sirex noctilio* control program in response to the 1987 Green Triangle outbreak. *Australian Forestry* 53: 33–40
- Healey S, Cohen W, Zhiqiang Y and Krankina O** (2005) Comparison of tasseled cap based Landsat data structures for use in forest disturbance detection. *Remote Sensing of the Environment* 97: 301–310
- Ismail R, Brink A, Verleur M and Boreham G** (2005) An integrated approach to managing *Sirex noctilio* infestations. *The Leaflet (Sappi forest quarterly newsletter)* 41: 7
- Ismail R, Mutanga O and Bob U** (2006) The use of high resolution airborne imagery for the detection of forest canopy damage by *Sirex noctilio*. In: Langin PA and Antonides MC (eds), *Precision forestry in plantations, semi-natural areas and natural forest: proceedings of the International Precision Forestry Symposium*. Stellenbosch University, South Africa, pp 119–134
- Jackson R** (1983) Spectral indices in n-space. *Remote Sensing of the Environment* 13: 409–421
- Jackson RD and Huete AR** (1991) Interpreting vegetation indices. *Preventative Veterinary Medicine* 11: 185–200
- Jin S and Sader S** (2005) Comparison of time series tasseled cap wetness and the normalised moisture index in detecting forest disturbances. *Remote Sensing of the Environment* 94: 364–372
- Jordan CF** (1969) Derivation of leaf area index from quality of light on the forest floor. *Ecology* 50: 663–666
- Lawrence RL and Labus M** (2003) Early detection of Douglas-fir beetle infestation with subcanopy resolution hyperspectral imagery. *Western Journal of Applied Forestry* 18(3): 1–5
- Leckie DG, Cloney E and Joyce S** (2005) Automated detection and mapping of crown discoloration caused by jack pine budworm with 2.5m resolution multispectral imagery. *International Journal of Earth Observation and Geoinformation* 7: 61–77
- Leckie DG, Jay C, Gougeon F, Sturrock R and Paradinee D** (2004) Detection and assessment of trees with *Phellinus weirii* (laminated root rot) using high resolution multi-spectral imagery. *International Journal of Remote Sensing* 25: 793–818
- Leckie DG, Teillet PM, Ostaff DP and Fedosjevs G** (1988) Sensor band selection for detecting current defoliation caused the spruce budworm. *Remote Sensing of Environment* 26: 31–50
- Leckie DG, Yuan X, Ostaff DP, Piene H and Maclean DA** (1992) Analysis of high resolution multispectral MEIS imagery for spruce budworm damage assessment on a single tree basis. *Remote Sensing of Environment* 40: 125–136
- Leica Geosystems** (2004) *Erdas Imagine® 8.7*. Leica Geosystems GIS and Mapping, Atlanta
- Lillesand T, Kiefer R and Chipman J** (2004) *Remote sensing and image interpretation*. John Wiley and Sons, New York. 763 pp
- MacFarlane D** (2004). *State of the environment report: Comrie-HCV areas & important rivers and streams*. Sappi, Pietermaritzburg
- McConnell TJ, Johnson EW and Burns B** (2000) A guide to conducting aerial sketchmapping surveys. *FHTET 00-001*., USDA Forest Service, Forest Health Technology Enterprise Team, Fort Collins, Colorado
- McGarigal K, Cushman S and Stafford S** (2000) *Multivariate statistics for wildlife and ecology research*. Springer, New York
- Mutanga O** (2005) Discriminating tropical grass canopies grown under different nitrogen treatments using spectra resampled to HYMAP. *International Journal of Geoinformatics* 1(2): 21–32

- Nelson RF** (1983) Detecting forest canopy change due to insect activity using Landsat MSS. *Photogrammetric Engineering and Remote Sensing* 49: 1303–1314
- Neumann FG and Minko G** (1981) The Sirex woodwasp in Australian radiata pine plantations. *Australian Forestry* 44: 46–63
- Price KP and Jakubauskas ME** (1998) Spectral retrogression and insect damage in lodgepole pine successional forest. *International Journal of Remote Sensing* 19: 1627–1632
- Radeloff VC, Mladenoff DJ and Boyce MS** (1999) Detecting jack pine budworm defoliation using spectral mixture analysis. *Remote Sensing of the Environment* 69: 156–169
- Richards JA** (1993) *Remote sensing digital image analysis: an introduction*. Springer-Verlag, Berlin
- Rouse JW, Haas RH, Schell JA and Deering DW** (1973) Monitoring vegetation systems in the great plains with ERTS. *Third ERTS Symposium, NASA SP-351*. pp 309–317
- Runesson UT** (1991) Considerations for early remote detection of mountain pine beetle in green-foliaged lodgepole pine. PhD thesis, University of British Columbia, Canada
- Schmidt KS and Skidmore AK** (2001) Exploring spectral discrimination of grass species in African rangelands. *International Journal of Remote Sensing* 22: 3421–3434
- Sharma R and Murtha P** (2001) Application of Landsat TM tasseled cap transformation in detection of mountain pine beetle infestations. In: *Final Proceedings: 23rd Canadian Symposium of Remote Sensing (CASI)*, Quebec. Canadian Aeronautics and Space Institute, Quebec City [CD-Proceedings]
- Skakun RS, Wulder MA and Franklin SE** (2003) Sensitivity of the thematic mapper enhanced wetness difference index to detect mountain pine beetle red-attack damage. *Remote Sensing of the Environment* 86: 433–443
- Skidmore AK** (1999) Accuracy assessment of spatial information. In: Stein A, van der Meer F and Gorte B (eds) *Spatial statistics for remote sensing*. Kluwer Academic Publishers, Netherlands. pp 197–209
- Slippers B, Coutinho TA, Wingfield BD and Wingfield MJ** (2003) A review of the genus *Amylostereum* and its association with woodwasps. *South African Journal of Science* 99: 70–74
- Stone C and Coops NC** (2004) Assessment and monitoring of damage from insects in Australian eucalypt forests and commercial plantations. *Australian Journal of Entomology* 43: 283–292
- Thenkabail P, Smith R and De Pauw E** (2002) Evaluation of narrowband and broadband vegetation indices for determining optimal hyperspectral wavebands for agricultural crop characterization. *Photogrammetric Engineering and Remote Sensing* 68: 607–621
- Tribe GD** (1995) The woodwasp *Sirex noctilio* Fabricius (Hymenoptera: Siricidae), a pest of *Pinus* species, now established in South Africa. *African Entomology* 3: 215–217
- Tribe GD and Cillie JJ** (2004) The spread of *Sirex noctilio* Fabricius (Hymenoptera: Siricidae) in South African pine plantations and the introduction and establishment of its biological control agents. *African Entomology* 12: 9–17
- Tucker CJ** (1979) Red and photographic infrared linear combinations for monitoring vegetation. *Remote Sensing of the Environment* 8: 127–150
- van Staden V, Erasmus BFN, Roux J, Wingfield MJ and van Jaarsveld AS** (2004) Modelling the spatial distribution of two important South African plantation forestry pathogens. *Forest Ecology and Management* 187: 61–73
- Vogelmann JE** (1990) Comparison between two vegetation indices for measuring different types of forest damage in the north-eastern United States. *International Journal of Remote Sensing* 11: 2281–2297
- Wingfield MJ, Roux J, Coutinho T, Govender P and Wingfield BD** (2001) Plantation disease and pest management in the next century. *Southern African Forestry Journal* 190: 67–71
- Wulder M, White J and Bentz B** (2004) Detection and mapping of mountain pine beetle red attack: matching information needs with appropriate remotely sensed data. In: *Proceedings from the Joint Annual Meeting of the Canadian Institute of Forestry and Society of American Foresters*. Society of American Foresters, Edmonton. pp 1–17
- Wulder MA and Dymond C** (2004) *Remote sensing in the survey of mountain pine beetle impacts: Review and recommendations*. Canadian Forest Service, Natural Resources, Victoria, Canada
- Yarbrough L, Eason G and Kuzmaul J** (2005) Tasseled cap coefficients for the QuickBird2 sensor: a comparison of methods and development. Presented at Pecora 16-American Society for Photogrammetry and Remote Sensing, October 23–27, Sioux Falls Convention Center, Sioux Falls, South Dakota. 10 pp, CD-ROM
- Yuan X, King DJ and Vlcek** (1991) Sugar maple decline assessment based on spectral and textural analysis of multispectral aerial videography. *Remote Sensing of the Environment* 37: 47–54
- Zwolinski JB, South DB and Droomer EAP** (1998) Pine mortality after planting on post-agricultural lands in South Africa. *Silva Fennica* 32: 271–280